

Riemann-Langevin Particle Filtering in Track-Before-Detect

Fernando J. Iglesias-Garcia, Pranab K. Mandal, Mélanie Bocquel, Antonio G. Marques

Abstract—Track-before-detect (TBD) is a powerful approach that consists in providing the tracker directly with the sensor measurements without any pre-detection. Due to the measurement model non-linearities, online state estimation in TBD is most commonly solved via particle filtering. Existing particle filters for TBD do not incorporate measurement information in their proposal distribution. The Langevin Monte Carlo (LMC) is a sampling method whose proposal is able to exploit all available knowledge of the posterior (that is, both prior and measurement information). This letter synthesizes recent advances in differential-geometric LMC-based filtering to introduce its application to TBD. The benefits of LMC filtering in TBD are illustrated in a challenging low-noise scenario.

Index Terms—particle filter, Langevin Monte Carlo, track-before-detect (TBD).

I. INTRODUCTION

SEQUENTIAL STATE estimation in nonlinear dynamical systems, such as tracking, is a challenging problem. Following a Bayesian approach, a closed-form expression of the posterior probability of the state is only attainable for a restricted class of models. Therefore, methods based on numerical approximations are oftentimes employed. Among these, Monte Carlo (MC) methods [1]–[3] are popular due to their flexibility and provable convergence guarantees. Particle filters (PFs) based on importance sampling (IS) are a straightforward implementation of MC methods in dynamical systems. However, their practical application is quickly challenged as the dimension of the state space increases. Moreover, IS-based PFs usually require resampling to avoid degeneracy, restraining their parallel implementation. Due to these limitations, the integration of Markov chain Monte Carlo (MCMC) in PF emerged as a competing alternative [4]–[7].

The main goal of this letter is to investigate the application of sequential differential-geometric MCMC-based PF to the problem of track-before-detect (TBD) [8]–[10]. In classical surveillance and tracking, the raw (video) data is preprocessed with a detection module and then, if necessary, passed on to the actual tracking module. As a result, if a dim object is not detected, it is also not tracked. On the other hand, TBD removes the detection stage and feeds the “unthresholded” image measurements directly into the tracker. In other

words, TBD performs *simultaneous* detection and tracking by integrating measurements over time and position, thereby allowing for higher detection probability of dim objects. Due to the non-linearities in TBD measurement models, PFs are commonly employed. Nevertheless, the proposal distributions in PFs (based on either MCMC or IS) developed for TBD have solely exploited the prior. This is, in general, inefficient and especially so, when the measurement noise is low, or equivalently, most of the posterior information is contained in the measurement. An MCMC based PF called the Langevin Monte Carlo (LMC) filter has been recently applied in the context of classical tracking [11]. The MCMC proposal of this filter exploits measurement knowledge through the Langevin equation [12]. One of the limitations of this LMC-PF is that it is parametrized by a step size that must be adjusted for every time step. Another drawback of the algorithm is that it approximates the gradient of the posterior and uses an MCMC-based PF methodology that introduces a bias [13]. The first limitation can be removed by using a differential-geometric Langevin proposal [14] and the second can be avoided by using a sequential MCMC approach [6]. A family of sequential MCMC filters leveraging differential geometry in the proposal has been more recently presented in [15], where the authors compared the performance of the filters in solving general filtering problems involving high-dimensional state vectors.

Through this letter we want to show that the TBD community can also benefit from the sequential MCMC based on a differential-geometric proposal, such as the Riemann-Langevin Monte Carlo (RLMC) filter. We would like to emphasize that the goal of the letter is not to compare all the different MC techniques there are. It is rather to show that in the TBD context an RLMC filter improves the tracking performance considerably, when compared with the other commonly used techniques. We do this by applying an RLMC filter, that is called the *simplified sequential manifold Metropolis-adjusted Langevin algorithm* (simplified SmMALA) algorithm in [15], to a TBD scenario with low measurement noise.

The rest of the letter is organized as follows. Section II reviews briefly the fundamentals of sequential MCMC and the Riemann-Langevin MC filter. We particularize in Section III the RLMC filter to our main focus area, TBD. The TBD model is described in Section III-A and the Riemann-Langevin proposal is explicitly derived in Section III-B. Using a low-noise TBD scenario as our testbed, we compare the performance of the RLMC filter to other existing methods. These numerical results are presented in Section IV. The conclusions in Section V close the letter.

Work in this paper was partially supported by the Spanish MINECO grants No TEC2013- 41604-R and TEC2016-75361-R, and the TRAX project from the Seventh Framework Programme under grant agreement N°607400.

F. Iglesias-Garcia and A. G. Marques are with the Department of Signal Theory and Communications, King Juan Carlos University.

M. Bocquel and P. K. Mandal are with the Faculty of Electrical Engineering, Mathematics, and Computer Science, University of Twente.

Manuscript received Month Day, 2018; revised Month Day, 2018.

II. PRELIMINARIES

In this section we briefly review why sequential MCMC [6] renders an efficient MCMC-based PF (Section II-A) and present the sequential RLMC filter (Section II-B) that we will implement. First, though, we introduce the basic notations used throughout the article.

Let \mathbf{s}_k and \mathbf{z}_k be the state and measurement vectors, respectively, at time step k , with the state transition density $p(\mathbf{s}_k|\mathbf{s}_{k-1})$ and the measurement likelihood $p(\mathbf{z}_k|\mathbf{s}_k)$. Given the sequence of measurements $\{\mathbf{z}_1, \dots, \mathbf{z}_k\} \equiv \mathbf{z}_{1:k}$, we denote the Bayesian posterior by $p(\mathbf{s}_k|\mathbf{z}_{1:k})$ and the prediction density by $p(\mathbf{s}_k|\mathbf{z}_{1:k-1})$.

A. Sequential MCMC

Recall that in MCMC-based particle filtering, after obtaining the new observation at each time step k , a Markov chain generates samples from the posterior. In the Markov chain, given the current state of the chain, \mathbf{s}_k^i , a new sample \mathbf{s}_k^* is drawn from a proposal distribution $q(\cdot|\mathbf{s}_k^i)$. Subsequently, an acceptance/rejection test is performed where the acceptance probability \mathcal{A} according to the Metropolis-Hastings algorithm is given by

$$\mathcal{A}(\mathbf{s}_k^i, \mathbf{s}_k^*) = \min \left\{ 1, \frac{p(\mathbf{z}_k|\mathbf{s}_k^*)p(\mathbf{s}_k^*|\mathbf{z}_{1:k-1})q(\mathbf{s}_k^i|\mathbf{s}_k^*)}{p(\mathbf{z}_k|\mathbf{s}_k^i)p(\mathbf{s}_k^i|\mathbf{z}_{1:k-1})q(\mathbf{s}_k^*|\mathbf{s}_k^i)} \right\}. \quad (1)$$

Clearly, unless the proposal is equal to the prediction density $p(\mathbf{s}_k|\mathbf{z}_{1:k-1})$, the computation of \mathcal{A} will require the evaluation of the latter, which is usually computationally expensive.

The sequential MCMC brings flexibility in choosing the proposal while maintaining efficient computation of the acceptance probability. The key is to first make, within one time-step of the Markov chain, a *joint* draw of the states at k and $k-1$ from the joint posterior $p(\mathbf{s}_k, \mathbf{s}_{k-1}|\mathbf{z}_{1:k})$ and then perform a *refinement* draw of \mathbf{s}_k to obtain samples from the required posterior $p(\mathbf{s}_k|\mathbf{z}_{1:k})$. An exploitation of the factorization of the joint density,

$$p(\mathbf{s}_k, \mathbf{s}_{k-1}|\mathbf{z}_{1:k}) \propto p(\mathbf{z}_k|\mathbf{s}_k)p(\mathbf{s}_k|\mathbf{s}_{k-1})p(\mathbf{s}_{k-1}|\mathbf{z}_{1:k-1}), \quad (2)$$

leads to more amenable acceptance probability calculations. In the joint stage, it only involves likelihoods. In the refinement stage, given a joint sample $(\mathbf{s}_k^\dagger, \mathbf{s}_{k-1}^\dagger)$, a new sample \mathbf{s}_k^* from the proposal $q(\cdot|\mathbf{s}_k^\dagger, \mathbf{s}_{k-1}^\dagger)$ is accepted with probability

$$\min \left\{ 1, \frac{p(\mathbf{z}_k|\mathbf{s}_k^*)p(\mathbf{s}_k^*|\mathbf{s}_{k-1}^\dagger)q(\mathbf{s}_k^\dagger|\mathbf{s}_k^*, \mathbf{s}_{k-1}^\dagger)}{p(\mathbf{z}_k|\mathbf{s}_k^\dagger)p(\mathbf{s}_k^\dagger|\mathbf{s}_{k-1}^\dagger)q(\mathbf{s}_k^*|\mathbf{s}_k^\dagger, \mathbf{s}_{k-1}^\dagger)} \right\}, \quad (3)$$

which involves the readily available transition density.

B. Sequential Riemann-Langevin Monte Carlo filter

Let us now summarize a sequential MCMC filter that uses the Riemannian manifold Langevin proposal q_{RL} in the refinement stage. This method is called *simplified SmMALA* in [15]. The exact form of the proposal (q_{RL}) will be presented in Section III-B, in the context of TBD. This proposal enables us to efficiently sample from the high-density regions of the state space leveraging the measurements.

Algorithm 1 describes the filter. The algorithm has an outer-most loop in k corresponding to the filtering time. The loop in i represents the evolution of the Markov chain in the MCMC. Regarding the rest of the symbols introduced in Algorithm 1: \hat{p} denotes the sample-based representation of a density; \sim denotes the action of sampling from a distribution, e.g. $u \sim \text{Unif}(0, 1)$ means that u is drawn from a continuous uniform $[0, 1]$; N_{bi} denotes the burn-in length; and N_p the number of particles.

Input : $\hat{p}(\mathbf{s}_0)$, $p(\mathbf{z}_k|\mathbf{s}_k)$, $p(\mathbf{s}_k|\mathbf{s}_{k-1})$, $\mathbf{z}_{1:K}$

Output: $\{\hat{p}(\mathbf{s}_k|\mathbf{z}_{1:k})\}_{k=1, \dots, K}$

```

1 for  $k = 1$  to  $K$  do
2    $(\mathbf{s}_k, \mathbf{s}_{k-1})^0 \sim p(\mathbf{s}_k|\mathbf{s}_{k-1})\hat{p}(\mathbf{s}_{k-1}|\mathbf{z}_{1:k-1})$ ;
3   for  $i = 0$  to  $N_{\text{bi}} + N_p - 1$  do
4     // Joint draw.
5      $(\mathbf{s}_k, \mathbf{s}_{k-1})^* \sim p(\mathbf{s}_k|\mathbf{s}_{k-1})\hat{p}(\mathbf{s}_{k-1}|\mathbf{z}_{1:k-1})$ ;
6      $\mathcal{A}(\mathbf{s}_k^i, \mathbf{s}_k^*) = \min \left\{ 1, \frac{p(\mathbf{z}_k|\mathbf{s}_k^*)}{p(\mathbf{z}_k|\mathbf{s}_k^i)} \right\}$ ;
7      $u \sim \text{Unif}(0, 1)$ ;
8     if  $u < \mathcal{A}(\mathbf{s}_k^i, \mathbf{s}_k^*)$  then
9        $(\mathbf{s}_k, \mathbf{s}_{k-1})^{i+1} = (\mathbf{s}_k, \mathbf{s}_{k-1})^*$ ;
10    else
11       $(\mathbf{s}_k, \mathbf{s}_{k-1})^{i+1} = (\mathbf{s}_k, \mathbf{s}_{k-1})^i$ ;
12    end
13    // Refinement.
14     $\mathbf{s}_k^* \sim q_{\text{RL}}(\mathbf{s}_k|\mathbf{s}_k^{i+1}, \mathbf{s}_{k-1}^{i+1}, \mathbf{z}_k)$ ;
15     $\mathcal{A}(\mathbf{s}_k^{i+1}, \mathbf{s}_k^*) =$ 
16     $\min \left\{ 1, \frac{p(\mathbf{z}_k|\mathbf{s}_k^*)p(\mathbf{s}_k^*|\mathbf{s}_{k-1}^{i+1})}{p(\mathbf{z}_k|\mathbf{s}_k^{i+1})p(\mathbf{s}_k^{i+1}|\mathbf{s}_{k-1}^{i+1})} \frac{q_{\text{RL}}(\mathbf{s}_k^{i+1}|\mathbf{s}_k^*, \mathbf{s}_{k-1}^{i+1}, \mathbf{z}_k)}{q_{\text{RL}}(\mathbf{s}_k^*|\mathbf{s}_k^{i+1}, \mathbf{s}_{k-1}^{i+1}, \mathbf{z}_k)} \right\}$ ;
17     $u \sim \text{Unif}(0, 1)$ ;
18    if  $u < \mathcal{A}(\mathbf{s}_k^{i+1}, \mathbf{s}_k^*)$  then
19       $\mathbf{s}_k^{i+1} = \mathbf{s}_k^*$ ;
20    end
21  end
22   $\hat{p}(\mathbf{s}_k|\mathbf{z}_{1:k}) = N_p^{-1} \sum_{i=N_{\text{bi}}+1}^{N_{\text{bi}}+N_p} \delta(\mathbf{s}_k - \mathbf{s}_k^i)$ ;
23 end

```

Algorithm 1: Riemann-Langevin MC filter.

III. RIEMANN-LANGEVIN PROPOSAL IN TRACK-BEFORE-DETECT

In this section we introduce the TBD model and derive the necessary equations to provide the exact form of the Riemann-Langevin proposal q_{RL} .

A. Track-before-detect measurement model

Recall that in TBD the tracker processes raw measurements. We consider the measurement model from [9], where an imaging sensor (e.g. camera, radar) measures the vector \mathbf{z}_k composed of the scalars $z_k^{(j)}$ in J pixels or cells:

$$\mathbf{z}_k = [z_k^{(1)} \dots z_k^{(J)}]^T. \quad (4)$$

The strength of the measured signal under the influence of an object with state-vector \mathbf{s} is assumed to be constant, denoted by A . Furthermore, we assume that the cell-measurement

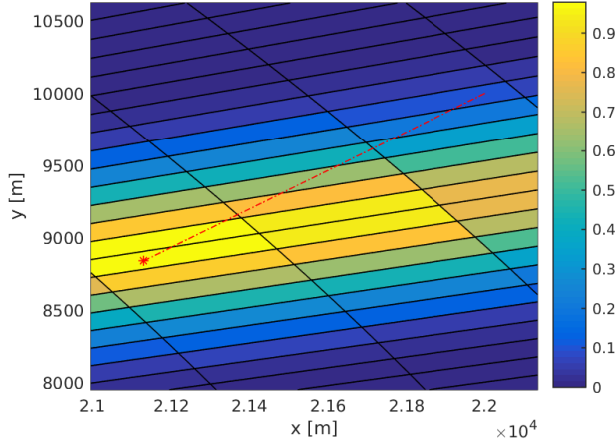


Fig. 1. Range-bearing imaging sensor grid, measurement, and object trajectory (dotted line) illustrating the TBD model. The solid lines depict the boundaries of the cells. The colors of the cells denote the measurements (5).

noises $w_k^{(j)}$'s are independent over the cells and are additive Gaussian with zero-mean and variance σ_w^2 , so that the signal-to-noise ratio (SNR) is $20 \log_{10} (A/\sigma_w)$. Then, the measurement in a single cell is given by

$$z_k^{(j)} = \hat{z}_k^{(j)} + w_k^{(j)} = A h^{(j)}(s_k) + w_k^{(j)}, \quad (5)$$

where $h^{(j)}$ is the *point spread function* characteristic of the sensor. A common choice for the point spread function [9], which we also use for the experiments in Section IV, is

$$h^{(j)}(s_k) = \exp \left(-\frac{(r_j - r(s_k))^2}{2R} - \frac{(b_j - b(s_k))^2}{2B} \right), \quad (6)$$

where r_j and b_j denote, respectively, the range and bearing cell centroids; $r(s_k)$ and $b(s_k)$ the position in polar coordinates; and R and B are sensing parameters that depend on the resolution and the boundaries of the surveillance area [9]. Other measurement dimensions (e.g. Doppler velocity, elevation) can be included in the point spread function depending on the type of imaging sensor. For illustration, Figure 1 shows a sensor grid and measurement following this model.

B. Riemann-Langevin proposal

The Riemann-Langevin proposal is used to draw the *refined* sample s'_k , given the current *joint* sample (s_k, s_{k-1}) . The general form of the proposal [15] is given by eqn. (12) at the bottom of this page. In the equation, $\nabla_x f(x)$ denotes the gradient-vector of f w.r.t. x and F is a metric tensor representing the Fisher information matrix [16]. In the sequential MCMC context, F becomes [15, eqn. (46)]:

$$\begin{aligned} F(s_k, s_{k-1}, z_k) &= -\mathbb{E}_{z_k|s_k} [\Delta_{s_k}^{s_k} \log(p(z_k|s_k)p(s_k|s_{k-1}))] \\ &= -\mathbb{E}_{z_k|s_k} [\Delta_{s_k}^{s_k} \log p(z_k|s_k)] - \Delta_{s_k}^{s_k} \log p(s_k|s_{k-1}) \end{aligned} \quad (7)$$

where $\mathbb{E}_{z_k|s_k}$ denotes the expected value w.r.t. $p(z_k|s_k)$ and $\Delta_x^x f(x)$ the Hessian of f w.r.t. x .

Similarly, the gradient in (12) can be written as:

$$\begin{aligned} \nabla_{s_k} \log(p(z_k|s_k)p(s_k|s_{k-1})) \\ = \nabla_{s_k} \log p(z_k|s_k) + \nabla_{s_k} \log p(s_k|s_{k-1}). \end{aligned} \quad (8)$$

We derive below the first terms in the right hand side of (8) and (7), involving the likelihood $p(z_k|s_k)$. The quantities corresponding to the state transition density can be obtained using the exact state-evolution model (see Section IV-A).

Note that the independence of the measurement noises over the cells leads to further simplification of the log-likelihood:

$$\log p(z_k|s_k) = \sum_{j=1}^J \log p(z_k^{(j)}|s_k). \quad (9)$$

According to (5), the cell-likelihood $p(z_k^{(j)}|s_k) \sim \mathcal{N}(\hat{z}_k^{(j)}, \sigma_w^2)$. Then, denoting $F(s_k, z_k) := -\mathbb{E}_{z_k|s_k} [\Delta_{s_k}^{s_k} \log p(z_k|s_k)]$, it follows (see, e.g., [17]) that

$$\nabla_{s_k} \log p(z_k|s_k) = \sum_{j=1}^J \frac{1}{\sigma_w^2} \left(\frac{\partial \hat{z}_k^{(j)}}{\partial s_k} \right)^T (z_k^{(j)} - \hat{z}_k^{(j)}), \quad (10)$$

$$F(s_k, z_k) = \sum_{j=1}^J \frac{1}{\sigma_w^2} \left(\frac{\partial \hat{z}_k^{(j)}}{\partial s_k} \right)^T \left(\frac{\partial \hat{z}_k^{(j)}}{\partial s_k} \right). \quad (11)$$

IV. NUMERICAL RESULTS

In this section, we describe the state evolution model and compare the performance of the Riemann-Langevin MC filter to the traditional bootstrap PF [1] and the standard sequential MCMC in a TBD application.

The reader may wonder about the choice of the RLMC filter (the SmMALA), instead of, for example, the Sequential manifold Hamiltonian Monte Carlo (SmHMC), which is also presented in [15] and outperforms the SmMALA in high dimensions. However, as we shall see below, we consider a 4-dimensional state-vector, and the experimental results in [14] and [15] show that the Langevin is generally more efficient than the Hamiltonian in low-dimensional state spaces (compare, e.g., Tables 3-7 with Table 10 in [14], or see [15, Table IV]).

A. Motion model

The scenario we consider is composed of a single object, moving along a straight-line at a constant speed of 180 kilometers per hour. The object trajectory lasts 30 seconds and is shown in Figure 1. Range and bearing measurements are reported by an imaging sensor every second (i.e., sampling time $\Delta_t = 1[s]$).

Thus the state vector is comprised of two-dimensional position (denoted by x and y) and the corresponding velocities: $s_k = [x_k \ \dot{x}_k \ y_k \ \dot{y}_k]^T$. The state evolution

$$q_{RL}(s'_k|s_k, s_{k-1}, z_k) = \mathcal{N} \left(s'_k; s_k + \frac{\epsilon^2}{2} F^{-1}(s_k, s_{k-1}, z_k) \nabla_{s_k} \log(p(z_k|s_k) p(s_k|s_{k-1})), \epsilon^2 F^{-1}(s_k, s_{k-1}, z_k) \right). \quad (12)$$

TABLE I
SENSOR PARAMETERS

Range PSF constant (R)	$1.56 \cdot 10^6 \text{ [m}^2\text{]}$
Bearing PSF constant (B)	$1.88 \cdot 10^{-4} \text{ [rad}^2\text{]}$
Range resolution	500 [m]
Bearing resolution	$5 \cdot 10^{-3} \text{ [rad]}$
Range lower bound	$22 \cdot 10^3 \text{ [m]}$
Range upper bound	$26 \cdot 10^3 \text{ [m]}$
Bearing lower bound	$-\pi/6 \text{ [rad]}$
Bearing upper bound	$\pi/6 \text{ [rad]}$

over time is given by a *nearly constant velocity* model [18]
 $\mathbf{s}_k = \mathbf{A} \mathbf{s}_{k-1} + \mathbf{v}_{k-1}$, with transition matrix

$$\mathbf{A} = \mathbf{I}_2 \otimes \begin{bmatrix} 1 & \Delta t \\ 0 & 1 \end{bmatrix} \quad (13)$$

where \otimes denotes the Kronecker product. The noise \mathbf{v}_k is Gaussian with zero mean and covariance

$$\mathbf{Q} = \begin{bmatrix} \sigma_{a_x}^2 & 0 \\ 0 & \sigma_{a_y}^2 \end{bmatrix} \otimes \begin{bmatrix} \Delta t^3/3 & \Delta t^2/2 \\ \Delta t^2/2 & \Delta t \end{bmatrix}, \quad (14)$$

where $\sigma_{a_x} = \sigma_{a_y} = 0.1 \text{ [m s}^{-2}\text{]}$ denote scalar standard deviations of the acceleration along the x and y axes, respectively.

With the Gaussian transition density, the quantities in (8) and (7), involving the state transition density and required for the RLMC proposal, can be obtained easily as:

$$\nabla_{\mathbf{s}_k} \log p(\mathbf{s}_k | \mathbf{s}_{k-1}) = -\mathbf{Q}^{-1} (\mathbf{s}_k - \mathbf{A} \mathbf{s}_{k-1}) \quad (15)$$

$$\Delta_{\mathbf{s}_k}^{\mathbf{s}_k} \log p(\mathbf{s}_k | \mathbf{s}_{k-1}) = -\mathbf{Q}^{-1}. \quad (16)$$

B. Measurement model and sensor parameters

The TBD measurement model is described in Section III-A. The specification of the parameters follows. The measurement noise is $\sigma_w = 10^{-4}$ and the SNR = 80 [dB], simulating a very low-noise scenario especially challenging for PF. The sensor parameters are listed in Table I. Figure 1 depicts the sensor grid in a region of the field-of-view as well as a sample measurement.

C. Compared methods and initialization

We compare the following methods:

- 1) The Riemann-Langevin MC filter.
- 2) The bootstrap PF based on IS and resampling.
- 3) Sequential MCMC with prior proposal.

The Riemann-Langevin MC filter uses 400 particles, the bootstrap PF 5000, and the sequential MCMC with prior proposal 3000. For both MCMC methods the burn-in length is 100. Initial particles are drawn from two uniform distributions: for the position the area of the distribution is $1 \text{ [km}^2\text{]}$; and for the velocity it is $100 \text{ [m}^2 \text{ s}^{-2}\text{]}$. Both distributions are centered around the ground truth.

D. Simulation results

The root mean squared error (RMSE) of the position estimate (x and y axes) is shown in Figure 2. Results are obtained averaging $N_{MC} = 50$ MC simulations. In all methods the estimated positions are given by the sample average over the population

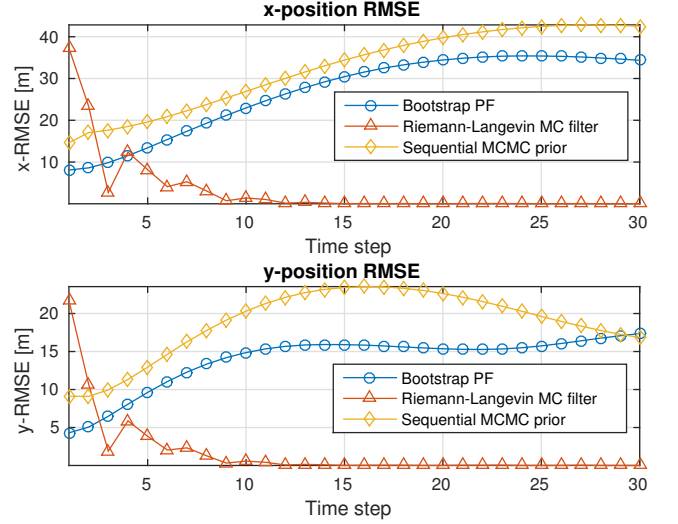


Fig. 2. Root mean squared error (RMSE) in the position state variables obtained with each of the methods in comparison.

of particles (burn-in is discarded in the MCMC methods). The results show that the Riemann-Langevin MC filter outperforms the other methods despite its lower number of samples. Note that during the first few time steps the low performance of the Riemann-Langevin MC filter is due to its fewer number of particles. The superior overall performance stems from the Riemann-Langevin proposal, which leverages both prior and measurement information, whereas the proposals in the other methods only contain prior information.

In particular, the particle clouds in the Riemann-Langevin MC filter are diverse, whereas the particle clouds in the other methods are degenerated due to the low noise. The Riemann-Langevin proposal achieves diverse clouds via adaptation, focusing on the regions of the state space where most mass of the posterior density lies. A measure of the particles' degeneration (which is opposite to their dispersion) with straightforward interpretation is the number of distinct particles. Across all the MC runs, the minimum and maximum number of distinct particles at the last time step are: 363 and 384 (of 400 total) in the Riemann-Langevin MC filter; 4 and 8 (of 5000) in the bootstrap PF; 4 and 11 (of 3000) in the sequential MCMC with prior proposal.

V. CONCLUSION

This letter presented the application of a sequential differential-geometric MCMC-based PF to the problem of TBD. We derived the expressions for the gradient and the Fisher information matrix of the TBD measurement model to obtain the TBD Riemann-Langevin proposal. An experiment dealing with low-noise, a setup particularly challenging for PF, illustrated that the Riemann-Langevin MC filter outperformed the considered alternatives.

REFERENCES

- [1] N. J. Gordon, D. J. Salmond, and A. F. Smith, "Novel approach to nonlinear/non-Gaussian Bayesian state estimation," in *IEE Proceedings on Radar and Signal Processing*, vol. 140, no. 2. IET, 1993, pp. 107–113.
- [2] A. Doucet, N. de Freitas, and N. Gordon, *Sequential Monte Carlo methods in practice*. Springer-Verlag, 2001.
- [3] M. S. Arulampalam, S. Maskell, N. Gordon, and T. Clapp, "A tutorial on particle filters for online nonlinear/non-Gaussian Bayesian tracking," *IEEE Transactions on Signal Processing*, vol. 50, no. 2, pp. 174–188, 2002.
- [4] Z. Khan, T. Balch, and F. Dellaert, "MCMC-based particle filtering for tracking a variable number of interacting targets," *IEEE Transactions on Pattern Analysis and Machine Intelligence*, vol. 27, no. 11, pp. 1805–1819, 2005.
- [5] K. Smith, S. O. Ba, J.-M. Odobez, and D. Gatica-Perez, "Tracking the visual focus of attention for a varying number of wandering people," *IEEE Transactions on Pattern Analysis and Machine Intelligence*, vol. 30, no. 7, pp. 1212–1229, 2008.
- [6] S. K. Pang, J. Li, and S. J. Godsill, "Detection and tracking of coordinated groups," *IEEE Transactions on Aerospace and Electronic Systems*, vol. 47, no. 1, pp. 472–502, 2011.
- [7] M. Bocquel, F. Papi, M. Podt, and H. Driessen, "Multitarget tracking with multiscan knowledge exploitation using sequential MCMC sampling," *IEEE Journal of Selected Topics in Signal Processing*, vol. 7, no. 3, pp. 532–542, 2013.
- [8] D. Salmond and H. Birch, "A particle filter for track-before-detect," in *Proceedings of the American Control Conference*, vol. 5. IEEE, 2001, pp. 3755–3760.
- [9] Y. Boers and J. Driessen, "Multitarget particle filter track before detect application," in *IEE Proceedings Radar, Sonar and Navigation*, vol. 151, no. 6. IET, 2004, pp. 351–357.
- [10] M. G. Rutten, N. J. Gordon, and S. Maskell, "Recursive track-before-detect with target amplitude fluctuations," in *IEE Proceedings Radar, Sonar and Navigation*, vol. 152, no. 5. IET, 2005, pp. 345–352.
- [11] F. J. Iglesias García, M. Bocquel, and H. Driessen, "Langevin Monte Carlo filtering for target tracking," in *18th International Conference on Information Fusion*. IEEE, 2015, pp. 82–89.
- [12] S. Duane, A. D. Kennedy, B. J. Pendleton, and D. Roweth, "Hybrid Monte Carlo," *Physics letters B*, 1987.
- [13] F. J. Iglesias García, M. Bocquel, P. K. Mandal, and H. Driessen, "Acceptance probability of IP-MCMC-PF: revisited," in *10th Workshop on Sensor Data Fusion: Trends, Solutions, Applications*. IEEE, 2015.
- [14] M. Girolami and B. Calderhead, "Riemann manifold Langevin and Hamiltonian Monte Carlo methods," *Journal of the Royal Statistical Society: Series B (Statistical Methodology)*, vol. 73, no. 2, pp. 123–214, 2011.
- [15] F. Septier and G. W. Peters, "Langevin and Hamiltonian based sequential MCMC for efficient Bayesian filtering in high-dimensional spaces," *IEEE Journal of Selected Topics in Signal Processing*, vol. 10, no. 2, pp. 312–327, 2016.
- [16] S. Amari, *Differential-Geometrical Methods in Statistics*. Springer, 1985.
- [17] S. M. Kay, *Fundamentals of Statistical Signal Processing, Volume I: Estimation Theory*. Prentice Hall, 1993.
- [18] X. R. Li and V. P. Jilkov, "Survey of maneuvering target tracking. Part I. Dynamic models," *IEEE Transactions on Aerospace and Electronic Systems*, vol. 39, no. 4, pp. 1333–1364, 2003.